J Mol Model (2013) 19:321–328
DOI 10.1007/s00894-012-1539-4

ORIGINAL PAPER

A density functional theory analysis for the adsorption of the amine group on graphene and boron nitride nanosheets

Ernesto Chigo Anota · Alejandro Rodríguez Juárez · Miguel Castro · Heriberto Hernández Cocoletzi

Received: 24 April 2012 / Accepted: 16 July 2012 / Published online: 15 August 2012
© Springer-Verlag 2012

Abstract In this paper first principles total energy calculations to study the adsorption of amine group (NH_2) on graphene (G) and boron nitride (hBN) nanosheets are developed; the density functional theory, within the local density approximation and Perdew-Wang functional was employed. The sheets were modeled with a sufficiently proved C_nH_m-like cluster with armchair edge. The optimized geometry was obtained following the minimum energy criterion, searching on four positions for each nanosheet: perpendicular to the carbon atom, on the hexagon, inside the hexagon and on the bridge C–C, for the G-amine interaction; and, perpendicular to the B, perpendicular to the N, on the hexagon, and inside the hexagon, for the hBN-amine interaction. A physisorption, with amine parallel to the C–C–C bond with a distance graphene-amine of 2.56 Å, was found. For the case of BN a B–N bond, with bond length equal to 1.56 Å, was found; the amine lies perpendicular to the nanosheet. When the graphene is doped with B and Al atoms a chemisorption with B–N (1.57 Å) and Al–N (1.78 Å) bonds is observed; the bond angle in the amine group is also incremented, 5.5° and 8.1°, respectively. In the presence of point defects (monovacancies) of B in the hBN-amine and C in the G-amine, there exists chemisorption, increasing the reactivity of the sheets.

Keywords Amine · Boron nitride · CnHm clusters · DFT theory · Graphene

Introduction

The isolation of the graphene (G) in 2004 [1] and the hexagonal boron nitride (hBN) sheet in 2005 [2], have motivated many theoretical as well as experimental studies on these kind of structures, owing to their diversity of applications on chips [3] and biosensors [4], respectively. Main research has been directed to graphene, finding spectacular applications; however, with respect to the applications on the two dimensional (2D) hBN there is scarce knowledge. The similar atomic arrangement between these two systems seems to be transcendental for the applications of the 2D hBN. At the same time, the chemical modification of these surfaces generated new two-dimensional systems [5–12], which require investigations on their functionalization in order to improve their capabilities, searching for new applications. Recently, Zettl et al. [13] have reported a convenient, highly efficient, radical-based chemical approach to functionalize boron nitrides nanotubes (BNNTs) with amine groups via an aggressive non-equilibrium ammonia glow plasma treatment. This renders BNNTs highly dispersible in the common organic solvent chloroform. The efficient polymer functionalization of BNNTs has been shown in order to develop new devices like glucose biosensor [14] and white light emitters [15]; BNNTs based composite materials are now possible [16].

Experimentally speaking, it is easier to find 2D hBN than BNNTs; then, applications for the first case would be more direct than the second one. A specific usage of a system requires the comprehension of the related properties; thinking the BN nanosheets as a biosensor, it would be necessary

E. C. Anota (✉) · H. H. Cocoletzi
Facultad de Ingeniería Química,
Benemérita Universidad Autónoma de Puebla,
C.U. San Manuel.,
C. P. 72570, Puebla, Mexico
e-mail: echigoa@yahoo.es

A. R. Juárez
'Instituto de Física 'Luís Rivera Terrazas',
Benemérita Universidad Autónoma de Puebla,
Apartado Postal J-48,
Puebla 72570, Mexico

M. Castro
Departamento de Física y Química Teórica,
DEPg-Facultad de Química,
Universidad Nacional Autónoma de México,
Mexico, DF C.P. 04510, Mexico

to know its structural parameters and properties like chemical ones. Searching insights on the former, in this work, the structural and electronic properties of the graphene and boron nitride nanosheets functionalized with the amine group (G–NH_2 and hBN–NH_2, respectively), are reported. The study has been done within the density functional theory using a circular C_nH_m-like cluster as the model; this model has been shown to be enough to study the graphene [17, 18] and boron nitride sheets [19]. The main objective of the paper is to analyze, theoretically, the adsorption process of the amine group on the graphene and hexagonal boron nitride surfaces looking for an increase on their reactivity; the intrinsic systems and with point defects (monovacancies) were considered.

Methodological aspects

The clusters we used in the calculations contain 24 carbon and 12 hydrogen atoms for graphene, and a triad of 12-12-12 of boron-nitrogen-hydrogen atoms was used for hexagonal boron nitride. The following sites for the adsorption of NH_2 molecule were considered: **a**) on top of boron (B) in a perpendicular way (Fig. 1a), **b**) on top of nitrogen (N) in a perpendicular way (Fig. 1b), **c**) perpendicular to the sheet and inside of the central hexagon (Fig. 1c), and **d**) lying perpendicular to sheet and on top of central hexagon (Fig. 1d), for the adsorption on the boron nitride sheet; **a**) on top of carbon (C) in a perpendicular way (Fig. 2a), **b**) perpendicularly to the C–C bond (Fig. 2b), **c**) perpendicular to the sheet and inside of the central hexagon (Fig. 2c), and **d**) perpendicular to sheet and on top of the central hexagon (Fig. 2d), when the adsorption on graphene is treated. For the case of doping graphene with B (Fig. 2e) and Al (Fig. 2f), the amine group is perpendicular to the sheet. When the monovacancies on the hBN sheet were considered, the amine was placed 2 Å away (Fig. 6a). The initial distance G-amine and hBN-amine sheet was of 2.0 Å for all selected configurations. For each system, bond lengths and bond angles, dipole moments, and adiabatic adsorption energies were determined for the configurations of lowest energy.

The obtainment of non-complex frequencies was the criterion for the structural stability of the lowest energy

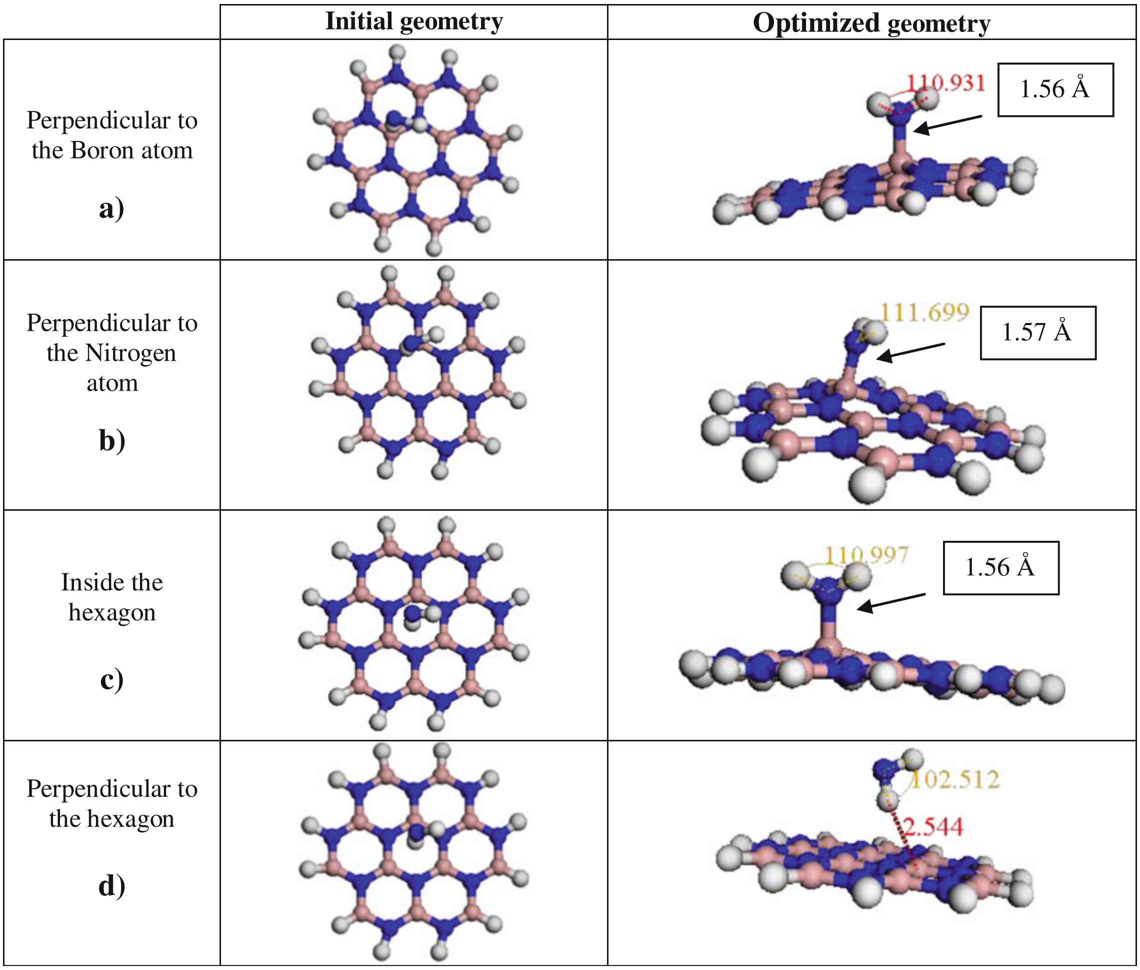

Fig. 1 Initial and final geometric configurations BN-amine interaction. In blue: N; pink: B; white: H

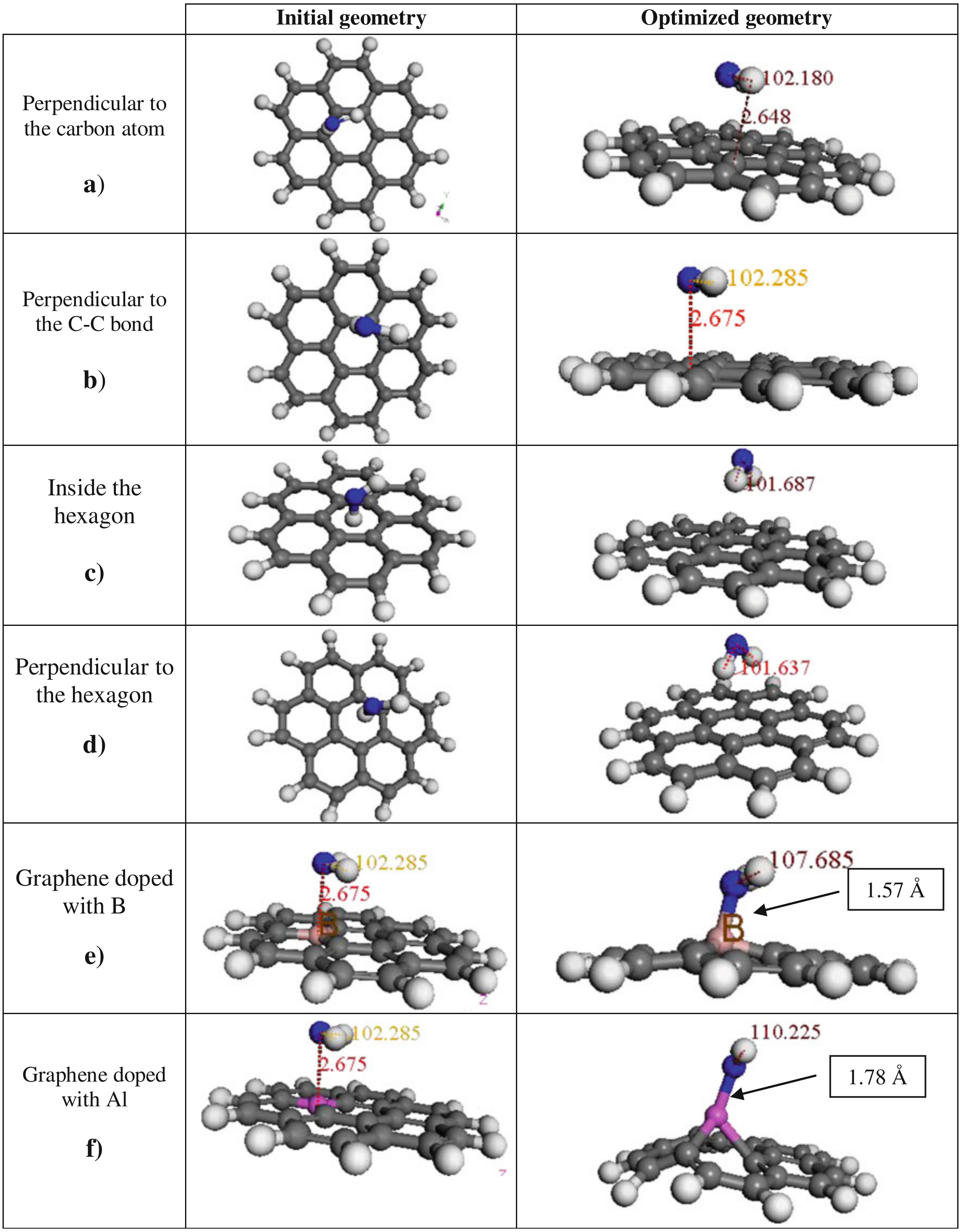

Fig. 2 Initial and final configurations for the G-amine and G+X-amine interactions; (X = B, Al). In gray: C; blue: N; white: H; pink: Al and orange: B

states of the clusters, which were determined through a full geometric optimization process, requiring that all atoms are allowed to relax [20]. Calculations were done within the DFT formalism, using the LDA approximation [21], as implemented in the quantum chemistry DMOL^3 code [22]; if the inclusion of spin does not affect the properties of the system, then it was not included in the calculations. The orbital basis set we used includes a *p* orbital for hydrogen atom, a *d* orbital for boron, carbon, nitrogen and aluminum atoms; neutral charge was required in all cases. The limit for orbitals was 0.41 nm and the convergence for the SCF cycles was 10^{-6} Ha. The cohesive energy for different graphene and boron nitride clusters, naphthalene and naphthalene like ($B_5N_5H_8$), phirene and phirene like ($B_8N_8H_{10}$), coronene and coronene like ($B_{12}N_{12}H_{12}$), and $C_{54}H_{18}$ and $B_{27}N_{27}H_{18}$ were calculated, obtaining the value of 3.82 [17] and 1.66 a.u./atom [23] for all of the systems, respectively, justifying from the energetic point of view the use of the armchair cluster as a model for these systems.

Results and discussion

Adsorption of NH_2 on boron nitride

The NH_2 radical on top of N provided the most stable configuration site, preserving its original orientation (perpendicular to the sheet), as confirmed by the total energy calculations (Fig. 1b). A Hirshfeld population analysis [24] shows a final positive charge for the amine, with a binding energy of −1.05 eV [25] which corresponds to a chemisorption like process; the new strong B-N bond (N of the amine group) formed has a bond length of 1.57 Å, a little bigger than that in reference [26], the B atom is attracted to the sheet inducing a protuberance which favors the adsorption. A similar value has been reported when the amine group is chemisorbed on BN nanotubes with different chiralities [27]. This originates different values on the B–N bond length on the sheet around the protuberance, 1.51, 1.51 and 1.54 Å. Something similar happens when chitosan is adsorbed on the (5,5) BN nanotubes, where a bond length of 1.69 Å was obtained [28]. The B–N bond length depends on the kind of structures which belong. The angle bond of the amine group when adsorbed on the sheet has a value of 9.54°, larger than that of the isolated molecule (102.15°, Table 1). The N–H bond length is reduced by 14 mÅ of its

Table 1 Bond distance, bond angles and adsorption energy for the optimal geometries

	Bond distance (Å)								Angle NH_2 (degree)	Adsorption energy (eV)
	N–H	B–N	C–C	C–N	B–N*	Al–N	B–C	Al–C		
NH_2	1.04								102.15	
BN		1.44								
G			1.42							
G+B			1.41				1.52 1.49			
G+Al			1.41			1.78 1.81				
$^{\zeta}$BN–NH_2	1.03	1.43^{+} 1.51^{++} 1.51^{++} 1.54^{++}			1.565				111.69	−1.05
$^{\zeta}$BN–NH_2 vacancy of B	1.03	1.40 1.42 1.43 1.44 1.46							108.67	−3.68
$^{\zeta}$G–NH_2	1.04		1.41	2.68					102.29	−0.32
$^{\zeta}$G–NH_2 vacancy of C	1.02		1.36 1.39 1.41 1.42 1.44 1.52	1.33					116.87	−5.19
$^{\zeta}$G+B–NH_2	1.03		1.42		1.573			1.56 1.56 1.54	107.69	−2.49
$^{\zeta}$G+Al–NH_2	1.02	1.36–1.43				1.778		1.94 1.93 2.06	110.23	−4.46

+Average value; ++ Value of the B–N bond when the amine is adsorbed;* New B–N bond; ζ using the stable configuration original value (1.04 Å); this means that the BN sheet induces a structural distortion on the amine group, larger than that observed on the adsorption of ozone and water on the same sheet [26, 27]. These changes originate a shift on the vibrational frequencies of the NH_2 group, which may be experimentally determined by infra-red photodissociation (IRPD), recently implemented [29]; it is important to note that a modification on the vibrational spectrum would be useful for sensing applications [18].

The dipole moment of the BN sheet (0 D) is incremented to 2.22 D when the NH_2 is adsorbed, a change from covalent to ionic character occurs; the vector is directed to the amine, something similar happens when the water molecule is adsorbed (2.47 D) [28]. The ozone molecule does not produce a significant change (0.79 D) on the hBN sheet [25]. The energy gap, defined as the difference of HOMO-LUMO, decreases from 5.17 eV to 0.58 eV, isolating system to semi-metal one. The chemical reactivity, obtained with the equation $\mu = (\text{HOMO} + \text{LUMO})/2$, decreases from −3.8 eV for the BN to −5.6 eV when the sheet is functionalized with the amine, which may be due to the planar geometry of the sheet, the contrary happens in the case of a tubular BN structure.

Figure 3 shows the molecular orbitals of the amine, the hBN sheet, and the hBN-amine systems. In the case of the hBN sheet the isosurfaces indicate that HOMO is mainly due to the p_z atomic orbitals of the nitrogen atom and to the p_z for the LUMO (Fig. 3b), in opposite direction. For the hBN-amine system, the p_z nitrogen orbitals of the sheet and the p_y nitrogen orbital of the amine contribute to the HOMO (Fig. 3c), as in the amine. The LUMO is mainly due to the orbital of the amine with a little presence of the p_z orbital of the sheet (Fig. 3a and c), which means that charge is mainly concentrated on the amine. An exothermic process occurs when a C replaces a B in the adsorption site, giving rise to an unstable system.

Adsorption of NH_2 on graphene

The lowest energy site happens when the amine group (with final negative charge) is in the C–C bond, the molecule is parallel to the graphene to a distance of 2.68 Å (Fig. 2b). The adsorption energy is of −0.32 eV, which corresponds to a physisorption process (Table 1), similar to the physisorbed ozone on graphene [25]; this value is lowest than the adsorption energy on the hBN-sheet, and to the water (directed to the sheet) on the same sheet [28]. The amine preserves its planar geometry.

The electronegativity of N motivated new research in order to functionalize graphene, both, experimentally and theoretically [30–35]. Moreover, Chi et al. [36] have shown that formaldehyde can be adsorbed on intrinsic and Al-doped graphene. Binding energies in the former case are of the order of meV, while in the latter case the energies are of the order of eV. It is evident that the adsorption energy is favored by the doping of the graphene layer. It seems that the functionalization of graphene with NH_2 would have better effects when it is doped with B and Al. Graphene remains planar when it is doped with a B atom on the minimum energy site, generating a little irregularity in the B–C bond lengths with values 1.56, 1.56 and 1.54 Å, on average; the B is immersed in the site where the amine is adsorbed inducing the chemisorption of this group (with positive final charge, Fig. 2c) with an adsorption energy of −2.49 eV (Table 1). The resulting B–N bond length is 1.573 Å, a little larger than that in the case when the amine is adsorbed on the hBN sheet. The doping also affects the angle formed in the amine, increased by 5.54°, with a N–H

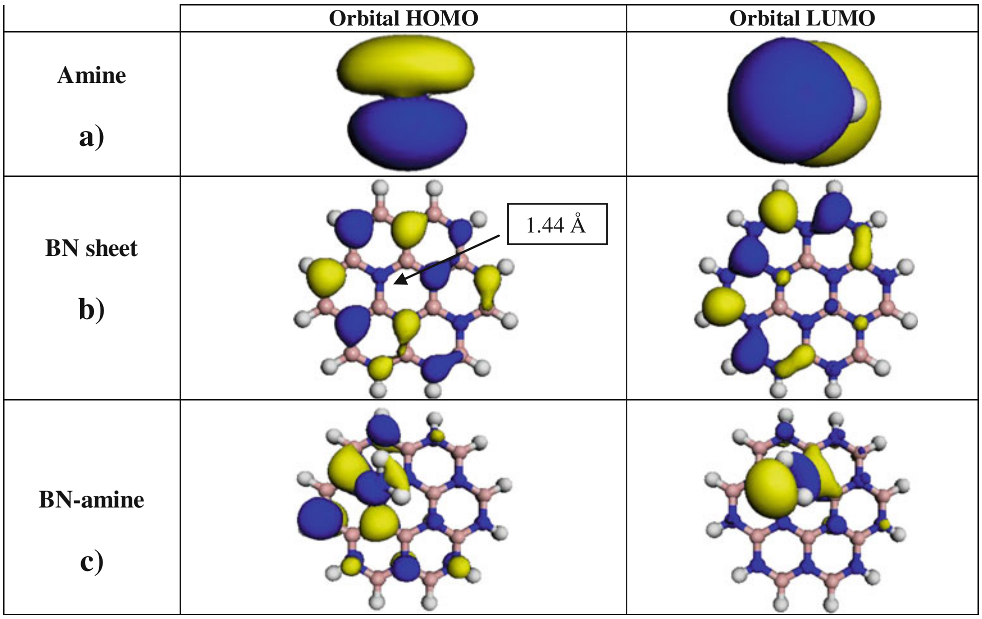

Fig. 3 HOMO and LUMO molecular orbitals for the NH_2, BN and BN-amine system. In blue the positive lobe and yellow the negative lobe

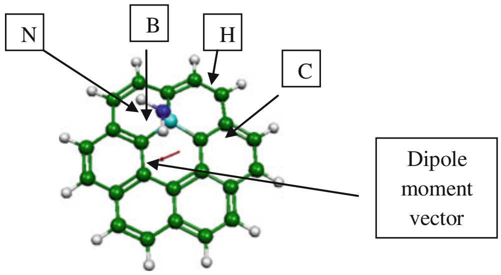

Fig. 4 Dipole moment vector for the system G+B-amine generated using the Gaussian package [49] and visualized by Molekel [50]

bond length of 1.04 Å. The Al atom is also chemisorbed on the optimized geometric position (the final charge of amine is negative, Fig. 2d), with an energy of −4.46 eV, generating a protuberance around the Al–N bond which has a bond length of 1.78 Å; different values for the Al–C are found, 1.94, 1.93 y 2.06 Å, similarly to the aluminum nitride sheet [37]. The angle in the amine is incremented by 8.1°.

The polarity of graphene is incremented from 0 D (covalent) to 0.56 and 0.84 D (a little ionic), when it is doped with B and Al, respectively. The dipole moment is a little augmented if the NH_2 is adsorbed, 0.84 D with B and 0.92 D with Al; the vector is pointing to the center of the hexagon (Fig. 4). The chemical potential of graphene (μ=−3.92 eV) increases when it is doped with B to −3.84 eV, and when it is doped with Al increases to −3.82 eV; when the amine is adsorbed, this quantity decreases to −4.53 eV, and to −4.54 in the presence of B and Al, respectively. The reactivity is also incremented when amine is adsorbed on the hBN sheet. The energy gap of the graphene has a value of 2.92 eV and when it is doped with B and Al, decreases to 2.54 eV and 1.85 eV, respectively; the presence of amine reduces the gap to 1.10 eV and 0.93 eV for B and Al, respectively.

The isosurfaces of the molecular orbitals show that for graphene the HOMO and the LUMO are mainly due to the

Fig. 5 HOMO and LUMO isosurfaces for G, G+B, G+Al, G-amine, G+B- amine and G+Al-amine

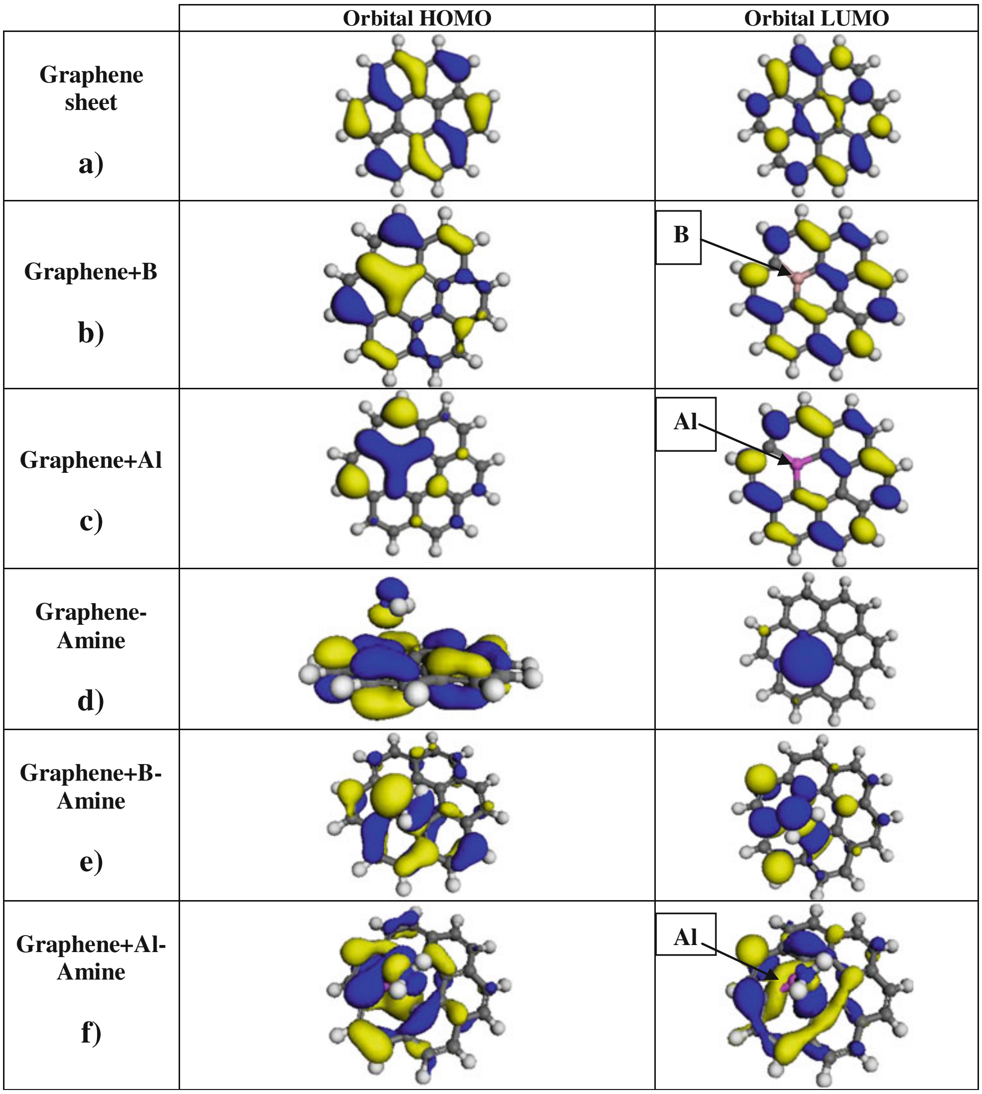

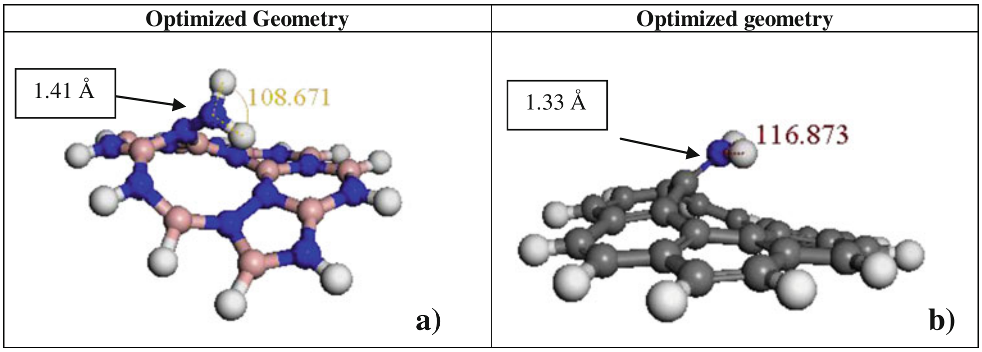

Fig. 6 Final geometries of BN-amine (**a**) and graphene-amine (**b**) systems with monovacancies of B and C, respectively

p_z with opposite direction, forming π molecular orbitals for the HOMO (Fig. 5a); when the amine is adsorbed p_y orbitals of the carbon (with π bonds) and p_y of the nitrogen conform the HOMO (Fig. 5d), such as in the isolated amine. The p_z of the B and C contributes to the HOMO when the graphene is doped with B and to the LUMO the p_z of the carbon and nitrogen (Fig. 5e). In the case of the doping with Al and the amine included, the p_y (π bonds formed) of C and the p_x of the amine constitute the HOMO and the LUMO, with the charge mainly distributed around the doping site (Fig. 5f). There exists a hybridization of the p_z of the B and the C (π bond) to form the HOMO (Fig. 5b) and the LUMO (Fig. 5b) is formed with p_z of the C for the system graphene-B. Something similar is found when the graphene is doped with Al (Fig. 5c).

Effects of vacancies on the adsorption of the amine group

The generation of point defects is an option to enhance the functionality of a surface; this has been done on graphene [38–43] and on hBN [44, 45]. We think, a monovacancy of C on graphene and monovacancies of B and N on hBN may change the adsorption capacity of these systems, we do that in this work. With the absence of a B atom in the sheet a new N–N bond is formed in the network (Fig. 6a) with a bond length of 1.41 Å with a hybridization sp^3; the angle in the amine is incremented from 102.15° to 108.67° and the N–H bond length is reduced only 0.011 Å. The stress on the bonds originates a reconstruction on the sheet forming a nonagon and a pentagon around the monovacancy forming a N–N bond with a bond length of 1.456 Å. The B–N bond length in the sheet is in the range 1.40 (pentagon) −1.46 Å (hexagon) due to the torsion suffered by the sheet. The adsorption energy of the amine is −3.68 eV, even lower compared with the intrinsic hBN (−1.05 eV); the same tendency is observed when chitosan is adsorbed on this sheet [46]. The energy gap reduces its value to 4.13 eV and the polarity has a value of 1.85 D, which means that the system remains as a semiconductor. The chemical reactivity increases (−3.37 eV), with respect to the BN sheet. The molecular orbitals show contribution of the p_x orbital of the amine and of the p_z of the nitrogen of the sheet to the HOMO; the LUMO has contribution of the p_z of the B and of the N of the sheet.

The vacancy generated in the graphene-amine system induces a reconstruction on the optimized geometry giving rise to a pentagon and a nonagon around the monovacancy (Fig. 6b). A new C–N bond is generated (1.33 Å) with hybridization sp^2. The C–C bond length has values from 1.36 to 1.52 Å, due to the curvature of the mesh. The bond angle in the amine (which is quimisorbed with energy −5.19 eV) is of 116.87° and the N–H bond length of 1.022 Å. The energy gap has the value 1.94 eV and the chemical reactivity is −3.29 eV, which means that the vacancy change graphene from conductor to a semiconductor and increases the reactivity. The dipole moment is 1.40 D. The atomic orbitals that mainly contribute to the HOMO are the p_x of the amine and the p_z of the carbon forming π bonds; the LUMO is formed with the p_z of the carbon and with the p_z of the amine.

Finally, when graphene is doped with N including the monovacancy, the amine is bonded to the nearest carbon with a bond length of 1.443 Å (Fig. 7) inducing a protuberance; the H–N–H angle increases by 9.32°, and the N–H bond length decreases by 0.018 Å. The dipole moment (0.74 D) is outward to the center of the hexagon and the chemical potential (−3.5 eV) indicates a reduction on the chemical reactivity.

Conclusions

The circular cluster model C_nH_m has permitted us to analyze the structural and electronic properties of the graphene and the two dimensional BN in the presence of the triatomic

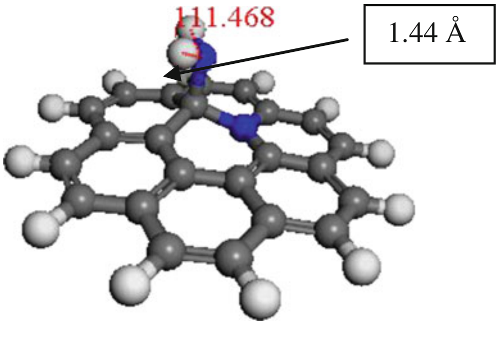

Fig. 7 Final configuration of interaction for G+N-amine. In gray:C; in white:H and in blue:N

amine group; the effect of the doping with B and Al was also studied. Results show that the adsorption mechanism is similar to that of the adsorption of water and ozone molecules on these systems, and that the angle in the amine increases with respect to the isolated one. At the same time, the capacity of the graphene to adsorb molecules of biological and industrial interest is clear. It is important to mention the little change in the polarity of the graphene when it is doped, but the big increase of this property on the BN. A considerable reduction of the gap is found, from semiconductor to a semimetal one; the chemical reactivity is also reduced, contrary to the tubular structures. The vacancies on the sheets increase the chemical reactivity, which may be useful in the design of electronic devices, and those involved in catalytic reactions free of metals, as proposed for N doped nanotubes [47] and nanosheets [48].

Acknowledgments This work was partially supported by projects: Vicerrectoria de Investigación y Estudios de Posgrado-Benemérita Universidad Autónoma de Puebla (CHAE-ING12-G), Cuerpo Académico Ingeniería en Materiales (BUAP-CA-177) and Consejo Nacional de Ciencia y Tecnología-México (No. 83982).

References

1. Novoselov KS, Geim AK, Morozov SV, Jiang D, Zhang Y, Dubonos SV, Grigorieva IV, Firsov AA (2004) Science 306:666–669
2. Novoselov KS, Jiang D, Schedin F, Booth TJ, Khotkevich VV, Morozov SV, Geim AK (2005) Proc Natl Acad Sci USA 102:10451–10453
3. Lin YM, Valdes Garcia A, Han SJ, Farmer DB, Meric I, Sun Y, Wu Y, Dimitrakopoulos C, Grill A, Avouris P, Jenkins KA (2010) Science 332:1294–1297
4. Pumera M (2011) Mater Today 14:308–315
5. Sofo JO, Chaudhari AS, Barber GD (2007) Phys Rev B 75:153401–153404
6. Wang WL, Kaxiras E (2010) New J Phys 12(125012):1–7
7. Nair RR, Ren WC, Jalil R, Diaz I, Kravets VG, Britnell L, Blake P, Schedin F, Mayorov AS, Yuan S, Katsnelson MI, Cheng HM, Strupinski W, Bulsheva LG, Okotrub AV, Grigoreva IV, Grigorenko AN, Novoselov KS, Geim AK (2010) Small 6(24):2877–2884
8. Wang Y (2010) Phys Status Solidi RRL 4:34–36
9. Yaya A, Ewels CP, Suarez-Martinez I, Wagner PH, Lefrant S, Okotrub A, Bulusheva L, Briddon PR (2011) Phys Rev B 83 (045411):1–5
10. Lew Yan Voon LC, Sandberg E, Aga RS, Farajian AA (2010) App Phys Lett 97(163114):1–3
11. Valentini L, Cardinali M, Kenny J M, Prato M, Monticelli O (2011) arXiv:1112.3459
12. Li B, Zhou L, Wu D, Peng H, Yan K, Zhou Y, Liu Z (2011) ACS Nano 5:5957–5961
13. Ikuno T, Sainsbury T, Okawa D, Frechet JMJ, Zettl A (2007) Solid State Commun 142:643–646
14. Wu J, Yin L (2011) ACS Appl Mater Interfaces 3:4354–4362
15. Gao Z, Zhi CH, Bando Y, Golberg D, Serizawa T (2011) ACS Appl Mater Interfaces 3:627–632
16. Zhi CH, Bando Y, Tang CH, Kuwahara H, Golberg D (2009) Adv Mater 21:2889–2893
17. Hernández Rosas JJ, Ramirez Gutierrez RE, Escobedo Morales A, Chigo Anota E (2011) J Mol Model 17(5):1133–1139
18. Rangel NL, Seminario GM (2008) J Phys Chem A 112:13699–13705
19. Chigo Anota E, Salazar Villanueva M, Hernández Cocoletzi H (2011) J Nanosci Nanotechnol 11(6):5515–5518
20. Foresman JB, Frisch Æ (1996) Exploring chemistry with electronic structure methods, 2nd edn. Gaussian Inc, USA, p 70
21. Perdew JP, Wang Y (1992) Phys Rev B 45:13244–13249
22. Delley B (1990) J Chem Phys 92:508–517
23. Chigo Anota E, Ramírez Gutierrez RE, Escobedo Morales A, Hernandez Cocoletzi G (2012) J Mol Model 18(5):2175–2184
24. Hirshfeld FL (1977) Theor Chim Acta B 44:129–138
25. Aguilar GG (1985) Adsorción y catálisis, ed. Universidad Autónoma de Puebla, México, pp 1–20
26. Chigo Anota E, Hernández Cocoletzi H, Rubio Rosas E (2011) Eur Phys J D 63:271–273
27. Cao F, Ren W, Ji Y, Zhao C (2009) Nanotechnology 20 (145703):1–7
28. Rodríguez Juárez A, Chigo Anota E, Flores Riveros A, Hernández Cocoletzi H (2012) DFT investigation of the adsorption of chitosan on BN nanotubes. J Mat Sci Eng: A (submitted)
29. Chigo Anota E, Salazar Villanueva M (2009) Sup y Vac 22(2):23–28
30. Jaegger TD, van Heinsbergen D, Klippenstein SJ, von Helden G, Meijer G, Duncan MA (2004) J Am Chem Soc 126:10981–10991
31. Wu T, Shen H, Sun L, Cheng B, Liu B, Shen J (2012) New J Chem 36:1385–1391
32. Zhao W, Höfert O, Gotterbarm K, Zhu JF, Papp C, Steinrück HP (2012) J Phys Chem C 116(8):5062–5066
33. Long D, Li W, Ling L, Miyawaki J, Mochida I, Yoon SH (2010) Langmuir 26(20):16096–16102
34. Usachov D, Vilkov O, Grüneis A, Haberer D, Fedorov A, Adamchuk VK, Preobrajenski AB, Dudin P, Barinov A, Oehzelt M, Laubschat C, Vyalikh DV (2011) Nano Lett 11(12):5401–5407
35. Chigo Anota E (2009) Sup y Vac 22(1):19–23
36. Chi M, Zhao YP (2009) Comput Mater Sci 46:1085–1090
37. Chigo Anota E, Salazar Villanueva M, Hernández Cocoletzi H (2010) Phys Status Solidi C 7:2252–2254
38. Gass MH, Bangert U, Bleloch AL, Wang P, Nair RR, Geim AK (2008) Nat Nanotechnol 3:676–681
39. Meyer JC, Kisielowski C, Erni R, Rossell MD, Crommie MF, Zettl A (2008) Nano Lett 8(11):3582–3586
40. Ugeda MM, Brihuega I, Guinea F, Gómez Rodríguez JM (2010) Phys Rev Lett 104(9)(096804):1–4
41. Bagri A, Mattevi C, Acik M, Chabal YJ, Chhowalla M, Shenoy VB (2010) Nat Chem 2:581–587
42. Banhart F, Kotakoski J, Krasheninnikov AV (2011) ACS Nano 5:26–41
43. Kotakoski J, Krasheninnikov AV (2011) Comput Nanosci 11:334–376
44. Alem N, Erni R, Kisielowski C, Rossell MD, Gannett W, Zettl A (2009) Phys Rev B 80(15)(155425):1–7
45. Lin Y, Williams TF, Cao W, Elsayed-Ali HE, Connell JW (2010) J Phys Chem C 114(41):17434–17439
46. Chigo Anota E, Escobedo Morales A, Hernández Rodríguez LD, Juárez Rodríguez A (2012) Observation of the chitosan adsorption on boron nitride nanosheets using the density functional theory. J Mat Sci Eng: A (submitted)
47. Van Dommels S, de Jong KP, Bitter JH (2006) Chem Commun 4859–4861
48. Long J, Xie X, Xu J, Gu Q, Chen L, Wang X (2012) ACS Catal 2:622–631
49. Frisch MJ, Trucks GW, Schlegel HB, Scuseria GE et al. (2009) Gaussian09, Revision C.01-SMP. Gaussian Inc, Pittsburgh
50. Portmann S (2002) Molekel version 4.3.win32